Determinant role of the edges in defining surface plasmon propagation in stripe waveguides and tapered concentrators

Johann Berthelot,[1] Francesco Tantussi,[2] Padmnabh Rai,[1] Gérard Colas des Francs,[1] Jean-Claude Weeber,[1] Alain Dereux,[1] Francesco Fuso,[2] Maria Allegrini,[2] and Alexandre Bouhelier[1,*]

[1]*Laboratoire Interdisciplinaire Carnot de Bourgogne, CNRS UMR 5209, Université de Bourgogne, 9 Avenue Alain Savary, Dijon, France*

[2]*CNISM and Dipartimento di Fisica "Enrico Fermi," Universitá di Pisa, Pisa, Italy*

**Corresponding author: alexandre.bouhelier@u-bourgogne.fr*

Received September 6, 2011; accepted November 3, 2011;
posted November 7, 2011 (Doc. ID 153674); published January 23, 2012

In this paper, we experimentally show the effect of waveguide discontinuity on the propagation of the surface plasmon in metal stripes and tapered terminations. Dual-plane leakage microscopy and near-field microscopy were performed on Au stripes with varied widths to image the surface plasmon intensity distribution in real and reciprocal spaces. We unambiguously demonstrate that edge diffraction is the limiting process determining the cutoff conditions of the surface plasmon mode. Finally, we determine the optimal tapered geometry leading to the highest transmission.

OCIS codes: 240.0240, 240.6680, 130.0130, 130.2790.

1. INTRODUCTION

The deployment of surface plasmon polariton-based devices for harnessing and controlling light in reduced dimensions is at the heart of the recent advances in nanophotonics. This interest emerged recently, because plasmonics offer the possibility to fabricate highly integrated, ultracompact photonic circuits and components [1–3], to achieve subwavelength dynamic localization of photon fields [4], or to control quantum emitters [5,6]. In functional plasmonic devices requiring the routing of surface plasmon polaritons (SPPs), practical realizations have been largely implemented on stripe [7–10] and dielectric-loaded surface plasmon waveguides [11–16]. These propagation media provide for a routine, cost-effective, controlled platform compared to more demanding approaches relying on chemically synthesized nanowires [17] or geometrical singularities [18,19]. Furthermore, launching surface plasmons in stripe waveguides is facilitated because the platform is compatible with common Kretschmann-type excitation schemes [7,20] or silicon-based photonic architecture [21].

The lateral confinement of the plasmon mode and its propagation in a stripe waveguide is strongly affected by the width of the structure [22,23]. Using near-field optical microscopy, Weeber *et al.* explained the intensity distribution of the fundamental plasmon mode in terms of coupling between the bound mode at the edges of the waveguide and the SPP at the metal/air interface, a picture departing from dielectric waveguide theory [23]. In a series of papers following, Zia *et al.* revisited these early conclusions by introducing a model consistent with ray optical interpretations [24,25]. They found that the reduction of SPP propagation for narrow stripe widths can be explained by introducing a radiation continuum formed by SPPs incident below the critical angle for total internal reflection [9]. While the effect of the edges is identified by these various authors [22–24] and significant interactions with the SPP mode were numerically predicted [24,26], it is not clear whether this dielectric discontinuity is necessary for defining the SPP cutoff conditions in these waveguide structures.

In this paper we present experimental evidence that the metal edges of the waveguide are providing for an additional radiative decay channel. By using dual-plane leakage radiation microscopy, we show that the SPP interaction with the edge occurrs at well-defined wave vectors. We also hypothesize that a hybridization of the plasmon mode with the bound edge mode is very inefficient, due to the large mismatch of their effective indices [27]. We therefore conclude that the propagation of SPPs in stripe waveguides deposited on a glass substrate is limited by an efficient directional leakage mechanism brought by the edges of the waveguide. A related consequence is that the transmission property of surface plasmon concentrators taking the form of a tapered termination is also affected by edge diffraction. Using near-field microscopy, we found that large taper angles are better suited for transmission than more acute geometries.

2. EDGE EFFECT IN SURFACE PLASMON STRIPE WAVEGUIDE

Gold waveguides were fabricated by standard electron-beam lithography and lift-off processes on an ITO-covered glass coverslip. The structure consists of an extented Au pad connected to waveguides of varying widths by 90° tapered funnels. The length of the waveguides was fixed at $L = 23\ \mu$m and the thickness of the Au layer at 50 nm. A scanning electron micrograph of the Au pad and the branching waveguides is shown in Fig. 1(a).

A p-polarized laser emitting at $\lambda = 800$ nm was used to excite surface plasmons in the Au pad using a high N.A. objective (N.A. = 1.49) in a Kretschmann-like configuration [28]. The radiative losses of the plasmon emitted in the substrate are

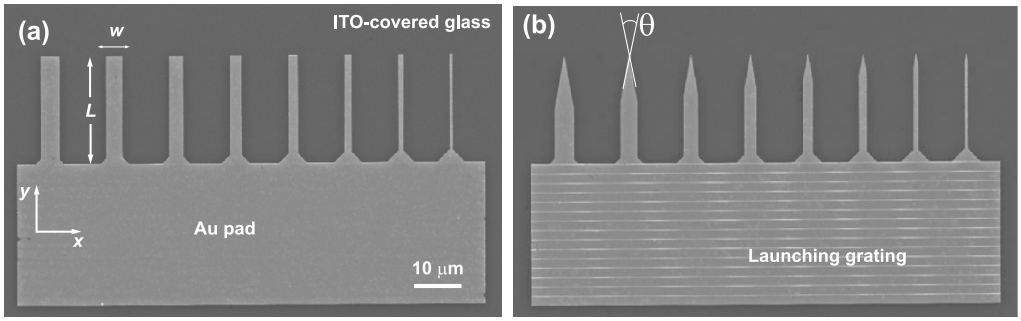

Fig. 1. Scanning electron micrograph of the SPP waveguides connected to a launching Au pad: (a) straight terminations, (b) tapered terminations with an angle of 20°. Note the grating used to excite the plasmon in (b) to circumvent the geometrical constraints of near-field imaging.

detected by the same objective [29] and are directed to two CCDs conjugated respectively with the image and Fourier planes of the microscope. The image plane information maps the plasmon intensity distribution in the stripe waveguide, while the Fourier plane renders the wave vector distribution [20]. Figure 2(a) shows typical leakage images of a surface plasmon propagating in an Au stripe for different width w. The launching site of the plasmon is located in the extended Au pad. During propagation the plasmon interacts with the edges by producing a high intensity located at either side of the metal structure, readily visible for the 1 μm wide stripe. This characteristic was recently observed on an isolated metal discontinuity and was attributed to a one-dimensional evanescent wave formed by conical diffraction of the SPPs at the edge [30]. At the extremity of the waveguide, the SPP mode is radiatively scattered out.

Figure 2(b) displays a partial image of the wave vector distribution limited to the range of interest. The incident wave vectors are confined in the region outlined by the white circle. The SPP signature is readily seen as a dark arc of circle within the illumination wave vectors and is understood in terms of destructive interference between the incident beam and surface plasmon leakages [31]. Because the illumination beam is weakly focused, SPPs in the Au pad are excited in a range of angle corresponding to the arc of circle present within the illumination momentum distribution. Quantitatively, the illumination beam launches SPPs propagating at $\pm 13°$ from the y axis.

The dynamic range of the image is encoded in a logarithmic scale to visualize the two bright lines situated at $k_y/k_o = 1.08$. These two lines are spanning the complete k_x/k_o axis, where k_o is the vacuum wave vector. These bright lines are the signature of a one-dimensional evanescent wave located in the superstrate and frustrated by the substrate [30]. Figure 2(b) unambiguously demonstrates that radiative diffraction by the edges occurs in the k_x/k_o plane around a vary narrow range of wave vectors limited to $\Delta k_y/k_o = 0.036$. The value of $\Delta k_y/k_o$ is given by the spread of wave vectors δk_{spp} coupled to the plasmon within the illumination area (dark arc of circle) and depends, therefore, on the excitation conditions. δk_{spp} also encodes all the different loss channels of the SPPs excited in the film and propagating in the stripe. Interestingly, we could not find any evidence in Fourier plane imaging of the light scattered at the end of the waveguide. At this location, the plasmon is simply scattered in a broad distribution of wave vectors in the substrate, which make it difficult to unambiguously measure. We have confirmed this on the large Au pad for a plasmon impinging normally on the edge (data not shown). No obvious signature was detected in Fourier imaging despite a bright intensity located at the edge observed in the image plane.

By conducting a systematic analysis for different waveguide widths, we found a relationship between the intensity of the lines observed in Fourier space and the linewidth of the surface plasmon δk_{spp}. Figure 3(a) illustrates the trend. The increase of the plasmon mode linewidth, encoding all possible losses, for narrow stripes is concomitant to an increased brightness of the line present in the Fourier plane. The intensity of the Fourier line integrated along the k_x/k_o axis was normalized to the maximum value measured for $w = 1$ μm, while all other experimental parameters were kept constant. For larger stripes $w > 2.5$ μm, δk_{spp} is almost constant, while

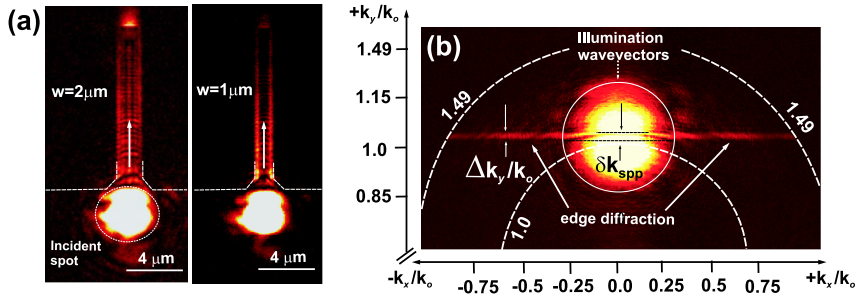

Fig. 2. (Color online) (a) Leakage images of a surface plasmon propagating in an Au stripe before being radiatively scattered out by the end face for $w = 2$ μm (left image) and $w = 1$ μm (right image). The interaction of the mode with the edges creates a high intensity region located at the discontinuity. (b) Partial Fourier plane image displaying the wave vector distribution corresponding to the $w = 1$ μm wide stripe. The maximum value (1.49) is given by the N.A. of the objective. The distribution of the illumination wave vectors is indicated by the dotted circle. The SPP signature is visible as a dark line within the illumination wave vectors. Interaction of the SPP with the edges is responsible for the two bright lines at a constant k_y/k_o value. Logarithmic color scale.

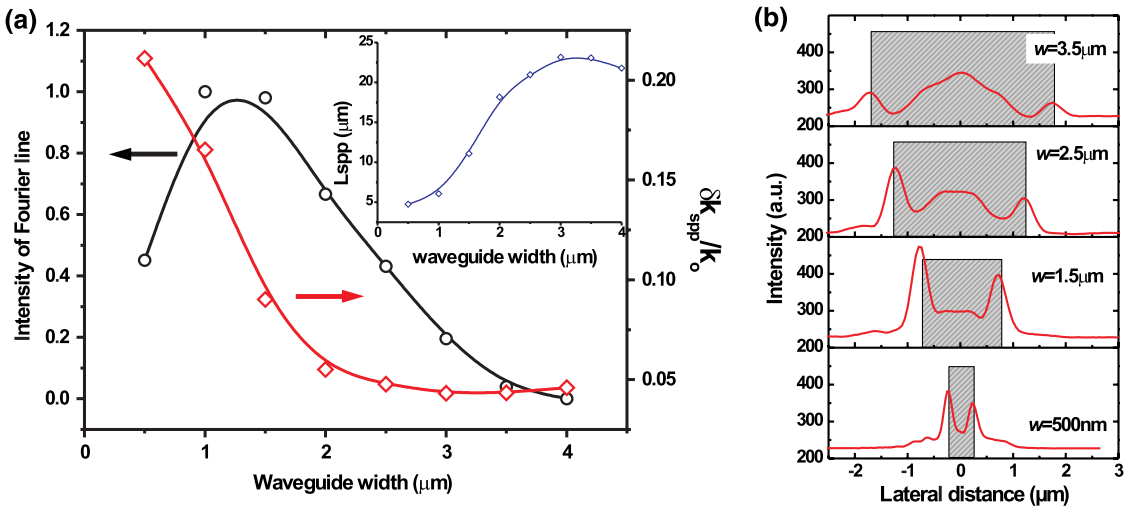

Fig. 3. (Color online) (a) Normalized intensity of the edge line extracted from Fourier plane analysis and measured surface plasmon width δk_{spp} as a function of the lateral dimension of the stripe waveguides. Inset: Propagation length L_{spp} inferred from δk_{spp}. (b) Intensity profiles taken along the x-direction at $y = 8$ μm from the excitation spot for various widths of the stripes. The physical footprint of the stripe is schematically represented by the shaded areas (off-scaled vertically for clarity).

the intensity of the Fourier line starts to increase for $w < 4$ μm. We explain this small difference with the following argument. δk_{spp} is measured at $k_x/k_o = 0$, that is, in the direction of propagation. SPPs travelling perfectly on-axis are therefore interacting weakly with the edges, and contributions in the Fourier line must originate for k_{spp} with an off-axis wave vector ($k_x/k_o \neq 0$). It is only for $w < 2.5$ μm that δk_{spp} is affected by the presence of the edges. The graph clearly indicates that edge diffraction introduces an additional radiative channel for width $w < 3$ μm. We were not able to observe any significant plasmon signature in the narrowest waveguide ($w = 0.5$ μm). The only contribution in the Fourier plane was the line resulting from its diffraction by the edges. Since the linewidth of the plasmon signature δk_{spp} directly encodes all possible losses, L_{spp} was evaluated by using the relation $L_{\mathrm{spp}} = 1/\delta k_{\mathrm{spp}}$, as shown in the inset of Fig. 3(a). From these two graphs, we therefore conclude that the SPP is predominantly attenuated in narrow stripe waveguides because of its diffraction at the edges along a well-defined k_x/k_o plane at $k_y/k_o = k_{\mathrm{spp}}$.

The cutoff behavior is illustrated by Fig. 3(b), showing intensity profiles extracted from image planes [Fig. 2(a)]. The lateral cross sections were taken along the x axis at $y = 8$ μm from the excitation spot. The footprint of the Au stripe is represented by the shaded areas (off-scaled vertically for clarity). For the widest stripe, the intensity profile is composed of a central maximum flanked by two peaks located at the edges of the stripe. The central maximum corresponds to the intensity distribution of the plasmon mode on the stripe, while the two side peaks result from edge diffraction of the mode. Because of the illumination symmetry, we do not anticipate higher-order modes to be efficiently excited [9]. The profile tends to indicate that intensity distribution corresponds to the fundamental mode.

We have confirmed the nature of the detected mode by computing the plasmon intensity for the considered geometry using a commercial mode solver (COMSOL Multiphysics, RF module). We have modeled infinitely long (two-dimensional) metallic stripes with a rectangular cross section deposited on a glass surface. COMSOL Multiphysics software is based on the finite element method, so that both the stripe and its surroundings need to be discretized. We used a circular computational window large enough to ensure convergency within a reasonable computing time (typically 7 to 10 μm) and imposed perfectly matched layer conditions at its boundary. To limit numerical difficulties, the stripe corners were rounded with a radius of curvature of 5 nm. The whole geometry (stripe and surroundings) was discretized using approximately 50,000 triangular meshes. Figure 4(a) shows the computed norm of the total electric field of the fundamental plasmon mode [9] in an (x, z) plane for a series of increasing widths. For waveguides with $w < 1$ μm, the SPP intensity significantly spread over the physical size of the stripes, clearly indicating a cutoff condition for $\lambda = 800$ nm, already reported in several studies [9,22,23]. What has not been carefully investigated, however, is the interaction of the SPP mode with the edges of the stripe. The insets of Fig. 4(a) are close-up views of the left-hand-side corner of the waveguide showing the confinement of the field at the discontinuity. This confirms the simple model discussed in Ref. [26]. By nature, SPPs cannot extend on regions without metal, as opposed to photonic mode that could extend outside the core waveguiding region. As a consequence, in the case of metal stripes with a width similar to or narrower than the SPP mode extension, the guided mode is strongly diffracted at the stripe edges. For comparison purposes, we have integrated the value of the field in a 27 nm × 27 nm area around the corners and plotted the results as a function of w in Fig. 4(b). The trend strongly resembles the measurement of Fig. 3(a), indicating that a large leakage intensity measured in the Fourier plane is indicative of a strong field amplitude located at the edges. For stripes larger than 2 μm, the SPP is reasonably confined by the gold structure and the electric field magnitude at the corner decreases with increasing w, a trend also measured in Fig. 3(a).

The computed electric field distributions of Fig. 4(a) significantly differ from the experimental leakage image displayed in Fig. 2(a), where the edge diffraction is a significant portion of the measured signal. The discrepancy originates from the

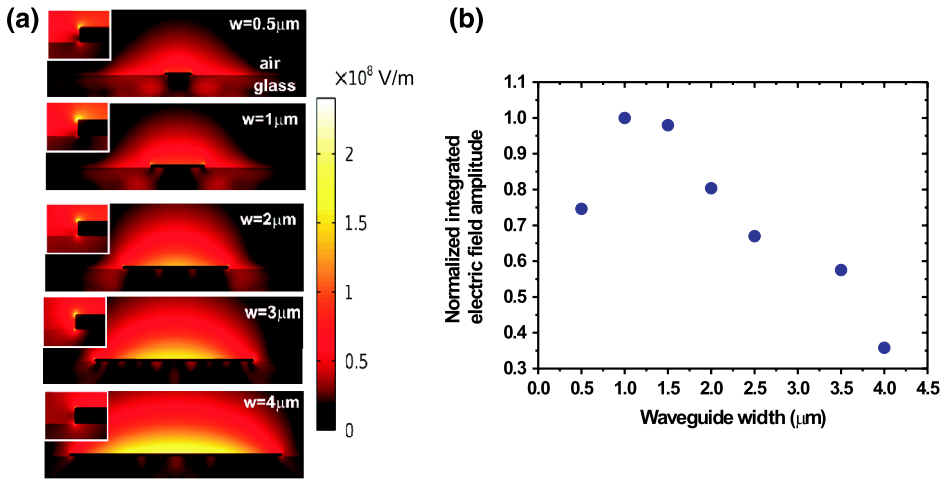

Fig. 4. (Color online) (a) Computed lateral distributions of the surface plasmon electric field for different widths w of Au stripe. $\lambda = 800$ nm, Au thickness $= 50$ nm. The insets display a magnified area around the left-hand-side corner. The high field magnitude located at the corner is readily visible. (b) Normalized electric field magnitude integrated in a 27 nm × 27 nm area around the corners as a function of waveguide width.

different planes of observation. Experimentally, the detected leakage of the plasmon field is strongly damped by the thickness of the metal layer. Therefore, the contribution stemming from edge diffraction emitted directly into the substrate has a comparable intensity to that of the plasmon mode. The same argument also explains why the rise of intensity located at the edge has not been observed by past near-field imaging [9,23], where the plasmon contribution was the largest.

3. TAPERED TERMINATIONS

Plasmon waveguides connected to tapered dielectric or metal structures are employed for adapting modes and efficiently exciting surface plasmon modes [13–33]. They are also used as a surface plasmon concentrator to focus the field at the apex of the termination [7,34,35]. In this section, we investigate the role of the opening angle of a tapered geometry in the concentration of the leaky surface plasmon mode as opposed to the bound mode existing at the glass/metal interface [33]. While leaky SPP modes are not suited for true nanoscale focusing [35], they may prove instrumental for locally addressing a desired area with SPPs without the constraints associated with the excitation of bound modes.

We have fabricated arrays of stripe waveguides where the width of the waveguide and the full angle of the taper θ was systematically varied from $\theta = 10°$ to $\theta = 90°$. An example of such an array is shown in Fig. 1(b). Here, all the waveguides end at a $\theta = 20°$ taper. We have used a combination of leakage radiation microscopy and near-field optical microscopy to extract the effect of the edge and determine the capacity of the tapers to concentrate the SPP field. Because of the constraints associated with near-field optical imaging, a grating was fabricated on the launching gold pad to excite the plasmon with a 850 nm beam incident from the air side at 36° from the normal.

Figure 5 shows a leakage radiation image of an SPP guided by 2 μm wide stripe terminated by tapers opened at 45° and 10°, respectively. A significant portion of the signal is scattered from the side edges of the taper. At first sight and as for SPP scattering at a straight termination [Fig. 2(a)], this signal should be distributed in a broad distribution of wave vectors, which would make it difficult to detect by Fourier imaging. Figure 5(b) shows the corresponding Fourier plane for the taper angled at 10°. Two inclined lines tilted 10° with respect to the k_y/k_o axis are readily visible, indicating that the rise of intensity along the lateral edges has a different origin than scattering at the physical end of the waveguide. It is therefore clear than the conical diffraction of the SPP with the edges of the taper significantly contributes to the SPP decay, thus decreasing the ability of the structure to focus the field efficiently.

To confirm this hypothesis, we have conducted near-field optical imaging of the extremity of the tapered waveguide. The SPP mode was launched with the help of the grating ruled on the extended gold pad. The polarization of an 850 nm laser diode was adjusted perpendicular to the grating in the direction of the waveguide. Figure 6 shows a series of topography and near-field optical images for a 3.5 μm wide stripe terminated by a 70° taper [Figs. 6(a) and 6(b)] and a 20° taper

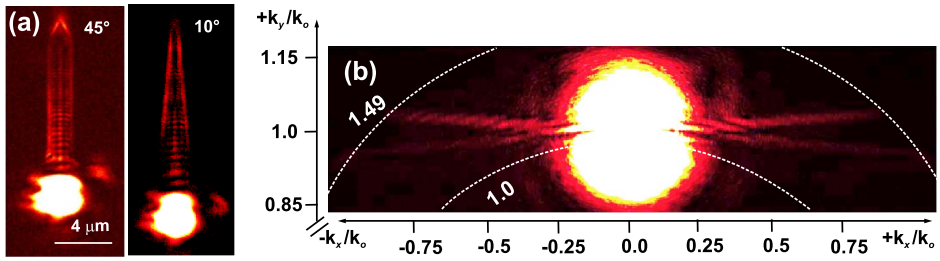

Fig. 5. (Color online) (a) Leakage images of a surface plasmon propagating in an Au stripe ($w = 2$ μm), terminated by a taper with an opening angle θ of 45° (left image) and 10° (right image), (b) corresponding partial Fourier plane $\theta = 10°$. Note the two inclined lines, the signature of diffraction at the edges of the taper.

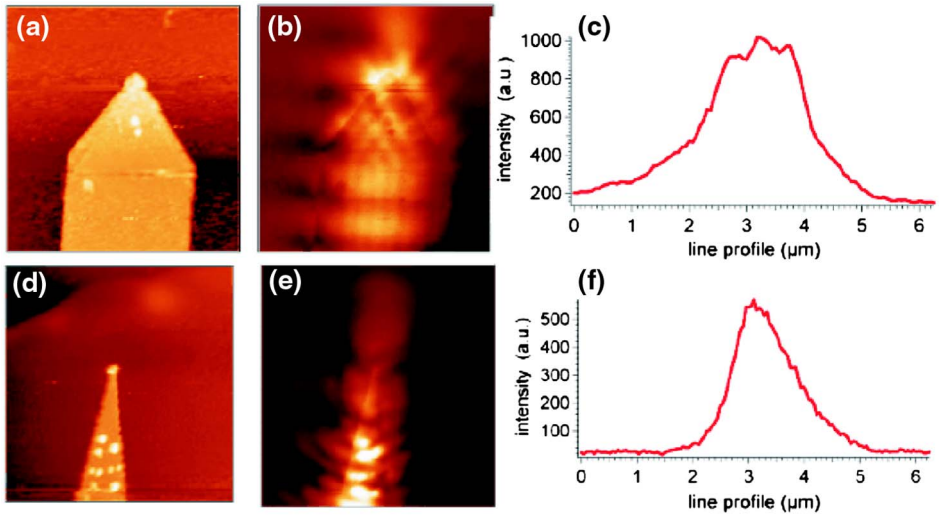

Fig. 6. (Color online) Near-field images of selected waveguides and tapers. (a) Topography of a 3.5 μm wide stripe terminated by a 70° taper, (b) corresponding near-field optical map, and (c) optical profile taken at the end of the taper in (b); (d) topography of a 3.5 μm wide stripe terminated by a 20° taper, (e) corresponding near-field optical map, and (f) optical profile taken at the end of the taper in (e).

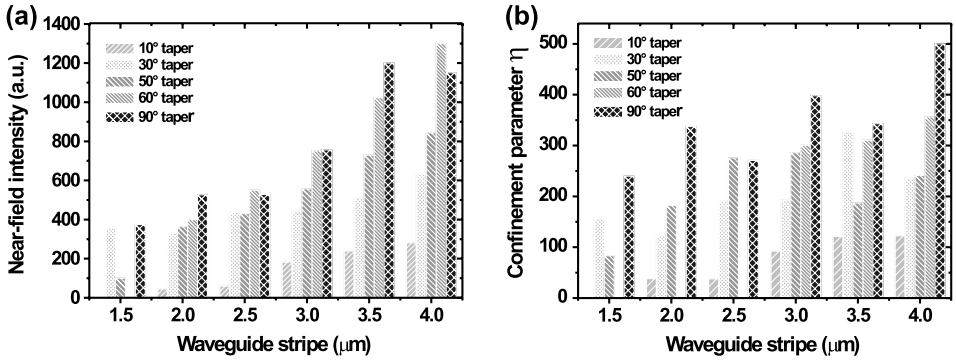

Fig. 7. (a) Near-field intensity measured at the taper extremity, (b) confinement parameter as a function of stripe width for different taper angles.

[Figs. 6(d) and 6(e)]. Near-field optical maps obtained at a regulated altitude of 2–3 nm reveal variations of intensity either related to the modal structure inside the taper [7] or to residues present on the surface. As already discussed above, the edges are not visible in the near-field optical maps, in agreement with previous observations [9,23], which is attributed to the large amplitude of the plasmon field in the stripe at this observation plane (see Fig. 4).

By measuring the detected near-field signal at the extremity of the tapers for all considered stripe widths [see, for instance, Figs. 6(c) and 6(f)], we have plotted the general capability of the termination to transmit the plasmon intensity in Fig. 7(a). As expected, for stripe widths above the cutoff, the intensity rises with opening angle and width of the structure. A high transmission, however, is generally not concomitant to an optimum confinement, as already alluded by the optical profiles in Figs. 6(c) and 6(f). In order to assess the focusing property of the tapers, we have defined a figure of merit, η, by dividing the near-field detected intensity by the FWHM of the intensity profile. Tapers with high transmission and low profile will consequently have the highest value of η. The analysis of η as a function of w and θ is shown in Fig. 7(b). Regardless of the stripe width, 90° tapers seem to offer a compromise between transmission of the SPP field and its concentration at the extremity. This is due to the degradation of the mode propagation by scattering along the stripe and the tapered edges.

4. CONCLUSION

In conclusion, we have unambiguously demonstrated the crucial role of the edges in defining the propagation of surface plasmons in a stripe waveguide. By conducting dual-plane leakage radiation microscopy, we have shown that edge diffraction gives rise to a high intensity located at the physical side of the waveguide. This signal, emitted in the substrate in a well-defined angular region, is an additional decay mechanism for the guided surface plasmon. Its weight increases when the stripe width decreases, thus providing experimental evidence for explaining cutoff behavior in this type of waveguiding structure. We have also investigated the potential use of tapered waveguide termination to concentrate laterally the surface plasmon mode present at the gold/air interface. After conducting a parametrical study for different widths of the stripe and opening angles of the terminations, tapers opened at 90° seem to provide for a relative optimum. This article emphasizes an aspect that has not be considered in-depth in the literature: the interaction of a surface plasmon with the physical edges of plasmonic devices should be taken into account when designing a plasmonic architecture.

ACKNOWLEDGMENTS

This work was partially funded by NanoSci E+ program under grant E^2-PLAS (ANR-08-NSCI-007), by MIUR through the PRIN project (2008J858Y7) "Plasmonics in metallic self-organized nanoparticles," and by the Agence Nationale de la Recherche (ANR) under grant Plastips (ANR-09-BLANC-0049-01).

REFERENCES

1. D. E. Chang, A. S. Sorensen, E. A. Demler, and M. D. Lukin, "A single-photon transistor using nanoscale surface plasmons," Nat. Phys. **3**, 807–812 (2007).
2. R. F. Oulton, V. J. Sorger, T. Zentgraf, R.-M. Ma, C. Gladden, L. Daia, G. Bartal, and X. Zhang, "Plasmon lasers at deep subwavelength scale," Nature **461**, 629–632 (2009).
3. D. K. Gramotnev and S. I. Bozhevolnyi, "Plasmonics beyond the diffraction limit," Nat. Photon. **4**, 83–91 (2010).
4. M. Aeschlimann, M. Bauer, D. Bayer, T. Brixner, F. J. G. de Abajo, W. Pfeiffer, M. Rohmer, C. Spindler, and F. Steeb, "Adaptive subwavelength control of nano-optical fields," Nature **446**, 301–304 (2007).
5. L. Novotny and N. F. Van Hulst, "Antennas for light," Nat. Photon. **5**, 83–90 (2011).
6. A. G. Curto, G. Volpe, T. H. Taminiau, M. P. Kreuzer, R. Quidant, and N. F. van Hulst, "Unidirectional emission of a quantum dot coupled to a nanoantenna," Science **329**, 930–933 (2010).
7. J.-C. Weeber, J. R. Krenn, A. Dereux, B. Lamprecht, Y. Lacroute, and J. P. Goudonnet, "Near-field observation of surface plasmon polariton propagation on thin metal stripes," Phys. Rev. B **64**, 045411 (2001).
8. J.-C. Weeber, M. U. González, A.-L. Baudrion, and A. Dereux, "Surface plasmon routing along right angle bent metal strips," Appl. Phys. Lett. **87**, 221101 (2005).
9. R. Zia, J. A. Schuller, and M. L. Brongersma, "Near-field characterization of guided polariton propagation and cutoff in surface plasmon waveguides," Phys. Rev. B **74**, 165415 (2006).
10. D. Koller, A. Hohenau, H. Ditlbacher, N. Galler, F. Reil, F. Aussenegg, A. Leitner, E. List, and J. Krenn, "Organic plasmon-emitting diode," Nat. Photon. **2**, 684–687 (2008).
11. B. Steinberger, A. Hohenau, H. Ditlbacher, A. L. Stepanov, A. Drezet, F. R. Aussenegg, A. Leitner, and J. R. Krenn, "Dielectric stripes on gold as surface plasmon waveguides," Appl. Phys. Lett. **88**, 094104 (2006).
12. B. Steinberger, A. Hohenau, H. Ditlbacher, F. R. Aussenegg, A. Leitner, and J. R. Krenn, "Dielectric stripes on gold as surface plasmon waveguides: bends and directional couplers," Appl. Phys. Lett. **91**, 081111 (2007).
13. T. Holmgaard, S. I. Bozhevolnyi, L. Markey, and A. Dereux, "Dielectric-loaded surface plasmon-polariton waveguides at telecommunication wavelengths: excitation and characterization," Appl. Phys. Lett. **92**, 011124 (2008).
14. T. Holmgaard, Z. Chen, S. I. Bozhevolnyi, L. Markey, A. Dereux, A. V. Krasavin, and A. V. Zayats, "Bend- and splitting loss of dielectric-loaded surface plasmon-polariton waveguides," Opt. Express **16**, 13585–13592 (2008).
15. J. Grandidier, S. Massenot, G. Colas des Francs, A. Bouhelier, J.-C. Weeber, L. Markey, and A. Dereux, "Dielectric-loaded surface plasmon polariton waveguides: figures of merit and mode characterization by image and fourier plane leakage microscopy," Phys. Rev. B **78**, 245419 (2008).
16. J. Grandidier, G. Colas des Francs, S. Massenot, A. Bouhelier, L. Markey, J.-C. Weeber, C. Finot, and A. Dereux, "Gain-assisted propagation in a plasmonic waveguide at telecom wavelength," Nano Lett. **9**, 2935–2939 (2009).
17. Y. Fang, Z. Li, Y. Huang, S. Zhang, P. Nordlander, N. J. Halas, and H. Xu, "Branched silver nanowires as controllable plasmon routers," Nano Lett. **10**, 1950–1954 (2010).
18. S. I. Bozhevolnyi, V. S. Volkov, E. Devaux, and T. W. Ebbesen, "Channel plasmon-polariton guiding by subwavelength metal grooves," Phys. Rev. Lett. **95**, 046802 (2005).
19. E. Moreno, S. G. Rodrigo, S. I. Bozhevolnyi, L. Martín-Moreno, and F. J. García-Vidal, "Guiding and focusing of electromagnetic fields with wedge plasmon polaritons," Phys. Rev. Lett. **100**, 023901 (2008).
20. S. Massenot, J. Grandidier, A. Bouhelier, G. Colas des Francs, L. Markey, J.-C. Weeber, A. Dereux, J. Renger, M. U. González, and R. Quidant, "Polymer-metal waveguides characterization by fourier plane leakage radiation microscopy," Appl. Phys. Lett. **91**, 243102 (2007).
21. R. M. Briggs, J. Grandidier, S. P. Burgos, E. Feigenbaum, and H. A. Atwater, "Efficient coupling between dielectric-loaded plasmonic and silicon photonic waveguides," Nano Lett. **10**, 4851–4857 (2010).
22. B. Lamprecht, J. R. Krenn, G. Schider, H. Ditlbacher, M. Salerno, N. Felidj, A. Leitner, F. R. Aussenegg, and J. Weeber, "Surface plasmon propagation in microscale metal stripes," Appl. Phys. Lett. **79**, 51–53 (2001).
23. J.-C. Weeber, Y. Lacroute, and A. Dereux, "Optical near-field distributions of surface plasmon waveguide modes," Phys. Rev. B **68**, 115401 (2003).
24. R. Zia, A. Chandran, and M. L. Brongersma, "Dielectric waveguide model for guided surface polaritons," Opt. Lett. **30**, 1473–1475 (2005).
25. R. Zia, M. D. Selker, and M. L. Brongersma, "Leaky and bound modes of surface plasmon waveguides," Phys. Rev. B **71**, 165431 (2005).
26. J. Grandidier, G. Colas des Francs, L. Markey, A. Bouhelier, S. Massenot, J.-C. Weeber, and A. Dereux, "Dielectric-loaded surface plasmon polariton waveguides on a finite-width metal strip," Appl. Phys. Lett. **96**, 063105 (2010).
27. P. Berini, "Plasmon-polariton waves guides by thin lossy metal films of finite width: bound modes of asymmetric structure," Phys. Rev. B **63**, 125417 (2001).
28. A. Bouhelier and G. P. Wiederrecht, "Surface plasmon rainbow jet," Opt. Lett. **30**, 884–886 (2005).
29. A. Bouhelier, T. Huser, H. Tamaru, H.-J. Güntherodt, and D. W. Pohl, "Plasmon transmissivity and reflectivity of narrow grooves in a silver film," J. Microsc. **194**, 571–573 (1999).
30. J. Berthelot, A. Bouhelier, G. Colas des Francs, J.-C. Weeber, and A. Dereux, "Excitation of a one-dimensional evanescent wave by conical edge diffraction of surface plasmon," Opt. Express **19**, 5303–5312 (2011).
31. H. Raether, *Surface Plasmons on Smooth and Rough Surfaces and on Gratings* (Springler-Verlag, 1988).
32. T. Holmgaard, S. Bozhevolnyi, L. Markey, A. Dereux, A. V. Krasavin, B. Bolger, and A. Zayats, "Efficient excitation of dielectric-loaded surface plasmon-polariton waveguide modes at telecommunication wavelengths," Phys. Rev. B **78**, 165431 (2008).
33. E. Verhagen, M. Spasenovic´, A. Polman, and L. K. Kuipers, "Nanowire plasmon excitation by adiabatic mode transformation," Phys. Rev. Lett. **102**, 203904 (2009).
34. M. I. Stockman, "Nanofocusing of optical energy in tapered plasmonic waveguides," Phys. Rev. Lett. **93**, 137404 (2004).
35. E. Verhagen, A. Polman, and L. Kuipers, "Nanofocusing in laterally tapered plasmonic waveguides," Opt. Express **16**, 45–57 (2008).